Journal of Medicinal Chemistry

ARTICLE

pubs.acs.org/jmc

# The Discovery of Phthalazinone-Based Human $H_1$ and $H_3$ Single-Ligand Antagonists Suitable for Intranasal Administration for the Treatment of Allergic Rhinitis

Panayiotis A. Procopiou,[*,†] Christopher Browning,[‡] Jennifer M. Buckley,[†] Kenneth L. Clark,[‡] Lise Fechner,[†] Paul M. Gore,[†] Ashley P. Hancock,[†] Simon T. Hodgson,[†] Duncan S. Holmes,[†] Michael Kranz,[∥] Brian E. Looker,[†] Karen M. L. Morriss,[†] Daniel L. Parton,[†] Linda J. Russell,[‡] Robert J. Slack,[‡] Steven L. Sollis,[†] Sadie Vile,[†] and Clarissa J. Watts[§]

[†]Departments of Medicinal Chemistry, [‡]Respiratory Biology, [§]Drug Metabolism and Pharmacokinetics, and [∥]Cheminformatics, GlaxoSmithKline Medicines Research Centre, Gunnels Wood Road, Stevenage, Hertfordshire, SG1 2NY, United Kingdom

S Supporting Information

**ABSTRACT:** A series of potent phthalazinone-based human $H_1$ and $H_3$ bivalent histamine receptor antagonists, suitable for intranasal administration for the potential treatment of allergic rhinitis, were identified. Blockade of $H_3$ receptors is thought to improve efficacy on nasal congestion, a symptom of allergic rhinitis that is currently not treated by current antihistamines. Two analogues (**56a** and **56b**) had slightly lower $H_1$ potency ($pA_2$ 9.1 and 8.9, respectively, vs 9.7 for the clinical gold-standard azelastine, and $H_3$ potency ($pK_i$ 9.6 and 9.5, respectively, vs 6.8 for azelastine). Compound **56a** had longer duration of action than azelastine, low brain penetration, and low oral bioavailability, which coupled with the predicted low clinical dose, should limit the potential of engaging CNS-related side-effects associated with $H_1$ or $H_3$ antagonism.

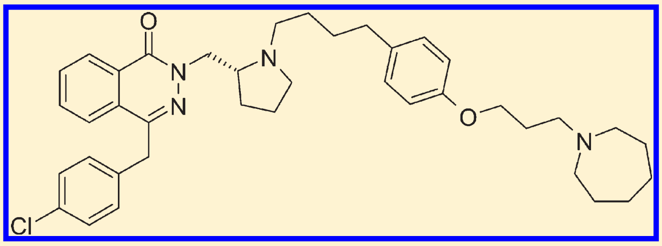


## 1. INTRODUCTION

Allergic rhinitis, also known as "hay fever," affects at least 10–25% of the world's population and has shown a steady increase in prevalence during the last 40 years.[1] The prevalence of allergic rhinitis may be significantly underestimated because of misdiagnosis, underdiagnosis, and failure of patients to seek medical attention. There are two types of allergic rhinitis, seasonal and perennial. The symptoms of seasonal allergic rhinitis include at the early stage nasal itching, irritation, and sneezing and at the late stage rhinorrhea and nasal congestion. The symptoms of perennial allergic rhinitis are similar, however, nasal congestion may be more pronounced. Either type of allergic rhinitis may also cause other symptoms such as irritation of the throat and/or eyes, epiphora, and edema around the eyes.[2] In addition to the classical symptoms, it is now recognized that allergic rhinitis has a significant impact on quality of life, such as social life, sleep disturbance as a result of nasal congestion, which in turn leads to reduced performance at work and school.[3] Allergic rhinitis and other allergic conditions are associated with the release of histamine from various cell types, but particularly mast cells.

The physiological effects of histamine are mediated by four major G-protein-coupled receptors, termed $H_1$, $H_2$, $H_3$, and $H_4$, which differ in their expression, signal transduction, and histamine-binding characteristics.[4] $H_1$ receptors are widely distributed throughout the CNS and periphery and play a critical role in regulating inflammatory responses and CNS activity such as wakefulness. $H_1$ antagonists, also known as $H_1$ blockers or antihistamines, are the most commonly used first-line medications for allergic rhinitis.[5,6] $H_2$ receptors regulate gastric acid secretion, and $H_2$ antagonists are used clinically to treat excess acid production and gastric ulceration.[7] The third histamine receptor subtype ($H_3$) is a presynaptic autoreceptor that controls the synthesis and release of histamine as well as other neurotransmitters such as acetylcholine, dopamine, GABA, glutamate, 5-HT, and noradrenaline.[8] Consequently, many applications have been proposed for $H_3$ receptor ligands, particularly in the CNS, where centrally acting $H_3$ antagonists may provide novel therapies for neurological disorders such as epilepsy, Parkinson's disease, Alzheimer's disease, attention-deficit hyperactivity disorder, sleep disturbances, cognition, schizophrenia, and obesity.[9−11] The more recently identified fourth receptor subtype ($H_4$) appears to be restricted to cells of the immune and inflammatory systems, and a physiological role for this receptor remains to be identified.[12]

First-generation $H_1$ receptor antagonists, while effective, caused sedation attributed to their ability to blockade $H_1$ receptors

Received: October 25, 2010
Published: March 07, 2011





dx.doi.org/10.1021/jm1013874 | J. Med. Chem. 2011, 54, 2183–2195

**Chart 1. Representative $H_1$ Receptor Antagonists Used Clinically**

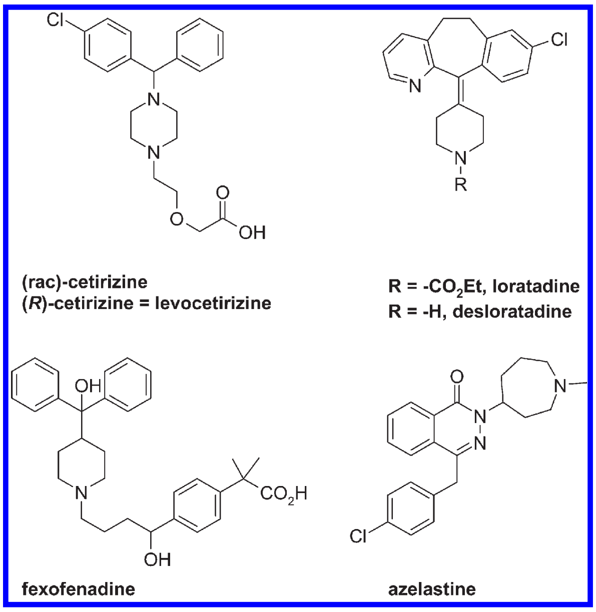


**Chart 2. Phthalazinone Template**

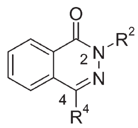

in the CNS. Second-generation $H_1$ receptor antagonists were developed with reduced CNS penetration and a corresponding reduction in the sedative side effects. Oral second-generation $H_1$ receptor antagonists such as cetirizine, desloratadine, fexofenadine, loratadine, and levocetirizine (Chart 1)[13] are effective in treating all the symptoms of allergic rhinitis apart from the nasal congestion. Hence they are often used in combination with α-adrenergic agonist decongestants such as pseudoephedrine. However, the use of α-adrenergic agonists is limited due to their potential to produce hypertension, agitation, and insomnia. In addition to the oral antihistamines, there are topical treatments available, such as azelastine nasal spray, which has been shown to benefit patients who have not responded adequately to loratadine and fexofenadine and is significantly more efficacious than cetirizine and levocabastine in patients with seasonal allergic rhinitis.[14,15]

Histamine $H_3$ receptors are expressed widely on both CNS and peripheral nerve endings and mediate the inhibition of neurotransmitter release.[8,16] Activation of $H_3$ receptor by histamine modulates outflow to resistance and capacitance vessels, causing vasodilation in rats,[17] guinea pigs,[18] and cats.[19] In vitro electrical stimulation of peripheral sympathetic nerves in isolated human saphenous vein[20,21] and porcine nasal mucosa[22] results in an increase in noradrenaline release and smooth muscle contraction, which can be inhibited by histamine $H_3$ receptor agonists such as (*R*)-α-methylhistamine. In addition, activation of $H_3$ receptors in isolated human nasal turbinate mucosa inhibits sympathetic vasoconstriction.[23] The same report also described high distribution of $H_3$ receptors in the human nasal mucosa. It is

**Scheme 1**[a]

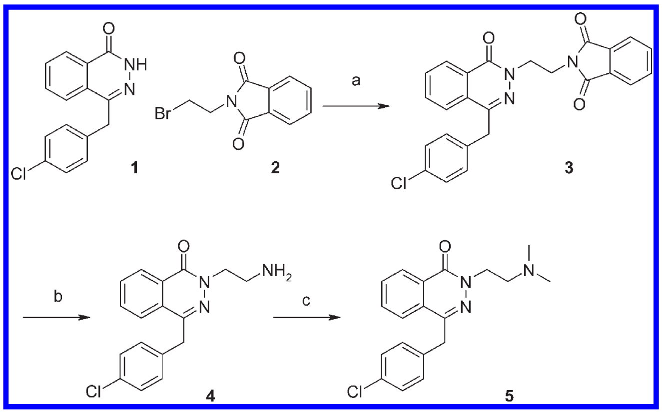


[a] Reagents and conditions: (a) NaH, DMF, 69%; (b) hydrazine hydrate, EtOH, reflux, 78%; (c) HCHO, $HCO_2H$, 100 °C, 55%.

**Scheme 2**[a]

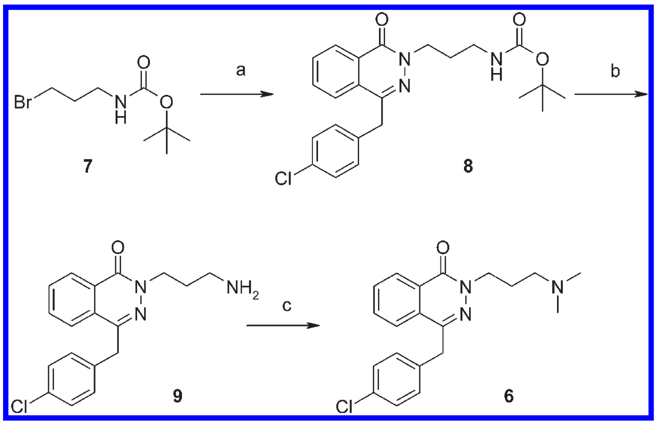


[a] Reagents and conditions: (a) **1**, NaH, DMF, 100%; (b) 4 M HCl-dioxane, 93%; (c) HCHO, $HCO_2H$, 100 °C, 90%.

thought that activation of the $H_3$ receptor on the presynaptic terminals of sympathetic neurones reduces noradrenaline release and this may contribute, together with the activation of the postsynaptic $H_1$ receptors, to the nasal blockage caused by histamine release. Consistent with this hypothesis, combination treatment of $H_1$ and $H_3$ antagonists have been shown to reverse the effects of mast cell activation on nasal airway resistance and nasal cavity volume in a cat model of nasal congestion in vivo.[24−26] Further evidence for the contribution of $H_3$ receptors to histamine-induced blockage of the nasal airway in normal healthy human volunteers was provided recently by acoustic rhinometry.[27] Scientists at the Schering-Plough Research Institute have published the first dual $H_1H_3$ receptor antagonist based on the first-generation $H_1$ antagonist chlorpheniramine and a 4-substituted imidazole with $H_1$ $K_i$ = 7 nM and $H_3$ $K_i$ = 15 nM.[28] In principle, there are two ways of targeting dual $H_1H_3$ pharmacology, either by using a combination of two individual selective antagonists or identifying a molecule that exhibits antagonism at both receptors. The former approach is easier to achieve but more expensive, as it requires the development and progression through expensive clinical trials of two chemical entities. We have examined both strategies, and in a recent paper we have reported our efforts in identifying a novel, nonbrain-penetrant histamine

Scheme 3[a]

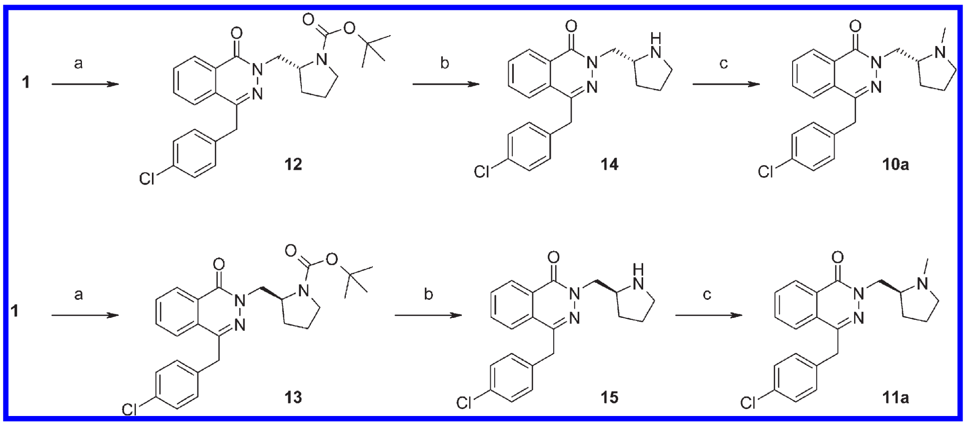


[a] Reagents and conditions: (a) diisopropyl azodicarboxylate, triphenylphosphine, THF, 80%; (b) 4 M HCl in dioxane, 90%; (c) HCHO, $HCO_2H$, reflux, 85%.

$H_3$ selective antagonist with optimized pharmacokinetic properties suitable for oral administration.[29] In this paper, we are reporting our efforts in identifying an $H_1H_3$ dual antagonist suitable for intranasal administration for the potential treatment of allergic rhinitis. Our efforts to identify an $H_1H_3$ dual antagonist suitable for oral administration will be reported in due course.[30]

## 2. OPTIMIZATION OF $H_1$ ANTAGONISM

Azelastine (Chart 1), a second-generation antihistamine, originally developed for oral administration but now also marketed for topical administration, is available as a racemic mixture. It is about 10 times more potent than the first-generation $H_1$ antagonist chlorpheniramine[31] and is oxidatively metabolized to an active metabolite, desmethylazelastine. Adverse effects of azelastine nasal spray include bitter taste (20%), somnolence (11%), and nasal burning (4%).[14,15] Azelastine was resolved, and the potency of its enantiomers was reported to be the same as that of the racemic mixture,[32] however, there are no reports associating the adverse effects of azelastine with one of its enantiomers. We established that the $H_3$ antagonism in dual $H_1H_3$ antagonists is tolerant to a range of structural modifications, whereas the $H_1$ antagonism is much more sensitive to variations. For this reason, we were interested in finding more potent homochiral phthalazinone analogues containing N2 substituents other than the azepine found in azelastine. Although the replacement of azelastine's azepine group with a 2-pyrrolidinomethyl group was reported to have led to increased in vivo activity in guinea pigs,[33] the effect of this group and that of its individual enantiomers on human cell lines was not reported. It was therefore decided to synthesize a variety of phthalazinone analogues with different N2-substituents in order to optimize the $H_1$ potency and then further optimize the phthalazinone C4 substituent before attempting the investigation of dual $H_1H_3$ antagonists (Chart 2).

**2.1. Chemistry.** The phthalazinone core (**1**)[34] was alkylated with *N*-(2-bromoethyl)phthalimide (**2**) in the presence of sodium hydride in DMF to give **3**, followed by deprotection with hydrazine hydrate to give **4** and Eschweiler−Clarke alkylation to provide the required dimethylaminoethyl derivative **5**[35] (Scheme 1). The homologous *N*,*N*-dimethylaminopropyl derivative **6** was prepared in a similar way from **1** and 3-[(*tert*-butoxycarbonyl)amino]propyl bromide (**7**), followed by deprotection of **8** to give **9** and Eschweiler−Clarke dimethylation (Scheme 2).

Scheme 4[a]

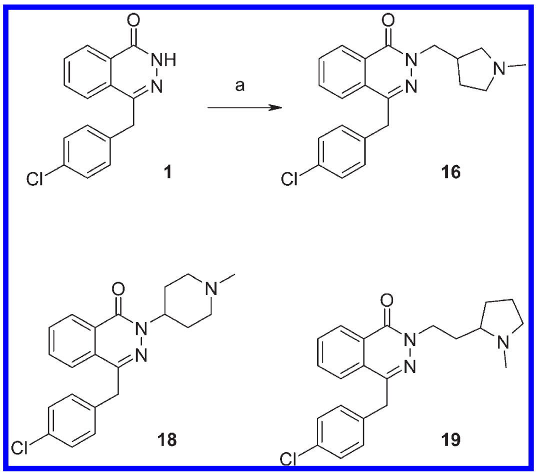


[a] Reagent and conditions: (a) (±)-(1-methyl-3-pyrrolidinyl)methanol (**17**), diisopropyl azodicarboxylate, $PPh_3$, THF.

The 2-pyrrolidinomethyl enantiomers **10a** and **11a** were synthesized from **1** and the appropriate Boc-protected prolinol using Mitsunobu conditions as shown in Scheme 3. The Mitsunobu condensation of **1** with (*S*)-(−)-2-(hydroxymethyl)-1-methylpyrrolidine was reported to give a mixture of the expected product and a rearrangement product due to formation of an aziridinium intermediate, which then ring-expanded.[36] Because this was due to the nucleophilicity of the pyrrolidine nitrogen, we envisaged using the Boc-protected prolinols, where the nucleophilicity of the nitrogen is reduced by the butoxycarbonyl group. The Mitsunobu couplings proceeded under these modified conditions in high yields and without any rearrangement to give **12** and **13**, respectively. Cleavage of the Boc protecting group with hydrogen chloride in dioxane gave the secondary amines **14** and **15**, and finally Eschweiler−Clarke methylation gave tertiary amines **10a** and **11a**.

The regioisomeric 3-pyrrolidinomethyl analogue **16** was prepared by Mitsunobu alkylation of **1** with (1-methyl-3-pyrrolidinyl)

Scheme 5[a]

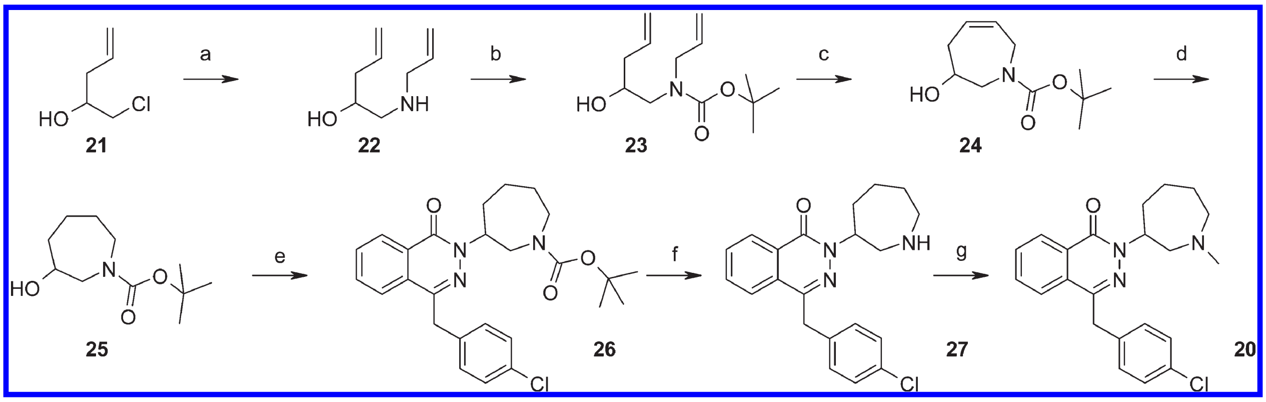


[a] Reagents and conditions: (a) allylamine, 87 °C, 60%; (b) $BOC_2O$, $Et_3N$, DCM, 91%; (c) Grubb's I catalyst, DCM, 40%; (d) $H_2$, $PtO_2$, EtOH, 100%; (e) **1**, di-*tert*-butyl azodicarboxylate, $PPh_3$, THF, 99%; (f) TFA, DCM, 82%; (g) HCHO, $HCO_2H$, 80 °C, 54%.

**Table 1. Phthalazinone C4-Substituents**

| R = | | R = | |
|---|---|---|---|
| **a** | 4-Cl-$C_6H_4CH_2$− | **j** | 3-F-$C_6H_4CH_2$− |
| **b** | 4-MeO-$C_6H_4CH_2$− | **k** | 3-Cl-$C_6H_4CH_2$− |
| **c** | 4-HO-$C_6H_4CH_2$− | **l** | 3-MeO-$C_6H_4CH_2$− |
| **d** | 4-EtO-$C_6H_4CH_2$− | **m** | 3-Me-$C_6H_4CH_2$− |
| **e** | 4-F-$C_6H_4CH_2$− | **n** | 3,4-F-$C_6H_4CH_2$− |
| **f** | 4-Me-$C_6H_4CH_2$− | **o** | 3,4-MeO-$C_6H_4CH_2$− |
| **g** | 4-*t*-Bu-$C_6H_4CH_2$− | **p** | c-$C_6H_{11}CH_2$− |
| **h** | 4-$MeO_2C$−$C_6H_4CH_2$− | **q** | $C_6H_5CH_2CH_2$− |
| **i** | 4-$HO_2C$−$C_6H_4CH_2$− | **r** | $CH_3CH_2CH_2CH_2CH_2$− |

methanol (**17**) without any rearrangements occurring, whereas the piperidine **18**[33] and pyrrolidinoethyl derivative **19**[34] were synthesized according to published procedures (Scheme 4).

The azelastine regioisomer **20** was prepared by the route outlined in Scheme 5. Chlorohydrine **21**[37] was heated in excess allyl amine to give **22**, which was converted to the Boc-protected amine **23**. Ring-closing metathesis of **23** with Grubbs I catalyst furnished the 5,6-olefin **24** as the major product, accompanied by the regioisomeric 6,7-olefin. Hydrogenation of **24** (and its regioisomer) provided **25**, which was then coupled to **1** using the Mitsunobu reaction. The resulting phthalazinone **26** was deprotected to azepine **27** and then reductively methylated to azelastine regioisomer **20**.

The C4-phthalazinone substituents (Table 1) were introduced in two ways. The first route was a linear route and is outlined in Scheme 6. Reaction between phthalic anhydride (**28**) and 4-methoxyphenylacetic acid (**29**) in the presence of sodium acetate gave **30**, which was treated with hydrazine to provide the phthalazinone **31**. Alkylation with *N*-Boc-D-prolinol using Mitsunobu conditions gave **32**, which was deprotected with TFA to **33** and then converted to the *N*-methyl derivative **10b** using Eschweiler−Clarke conditions. Reaction of **10b** with boron tribromide gave phenol **10c**, which was converted to the ethyl ether **10d** using the Mitsunobu reaction (Scheme 6).

The second route (Scheme 7) was a much more versatile route, suitable for array chemistry and allowing late-stage derivatization at C4. It started from the commercially available 4-chloro-1(2*H*)-phthalazinone (**34**), which was alkylated with *N*-Boc-D-prolinol under Mitsunobu conditions to provide **35**. Deprotection under acidic conditions provided **36**, which was then converted to the key intermediate **37** by Eschweiler−Clarke methylation. The required products **10** were obtained in one simple step by Negishi coupling, following treatment with a variety of organozinc reagents.

**2.2. Results and Discussion.** The affinity of compounds was evaluated in vitro at recombinant human histamine $H_1$ receptor in intact CHO cells by means of plate-based calcium imaging. Inhibition of agonist-induced cellular calcium mobilization was monitored using the calcium sensing dye Fluo-4AM in a FLIPR instrument.[38] The compounds were also evaluated in membranes from CHO cells transfected with cloned human histamine $H_3$ receptors for their ability to reduce histamine stimulated GTP-$\gamma$-S binding as determined by scintillation proximity detection. The adrenergic $\alpha_{1A}$ and $\alpha_{1B}$ receptor affinity of the test compounds was assessed in intact Ratl fibroblast cells by means of plate-based calcium imaging, and the data from all the above screens are summarized in Table 2. Azelastine was used as a standard, with affinities ($pK_i$) for $H_1$ and $H_3$ 8.9 and 6.8, respectively. The effect of the phthalazinone N2-basic amino group substituent (azepine, piperidine, pyrrolidine, or alkyl chain) was first examined, and the groups that had affinities for the $H_1$ receptor higher than that of azelastine were the two enantiomers of 2-pyrrolidinomethyl derivatives (**10a** and **11a**) and the simple *N*,*N*-dimethylaminoethyl derivative (**5**). It was apparent that a two-carbon chain between the point of attachment on the phthalazinone to the basic nitrogen (**5**, **10**) were preferred over the three-carbon analogues (**6**, **16**, **19**), whereas the piperidino analogue (**18**), being of intermediate length, showed similar affinity to azelastine. This is rationalized by comparing azelastine's binding in the $H_1$ homology model. This model was based on the bovine rhodopsin structure and was constructed well before the recently published X-ray crystal structures of a number of 7TM receptors. The basic nitrogen of azelastine was tethered to Asp-107 of the TM3,[39] allowing the bulk of the ligand to extend into the large pocket formed by TM3, TM4, TM5, and TM6 (Figure 1). Two Tyr side-chains from the opposing TM3 and TM6 were observed to interact with each other, thereby forming a channel between the ligand binding pocket and Asp-107. Both Tyr hydroxyl groups can form hydrogen bonds to the phthalazinone carbonyl in some of the low-energy conformations. The chlorobenzyl group reached between three aromatic rings of TM5 and TM6, thereby blocking

Scheme 6[a]

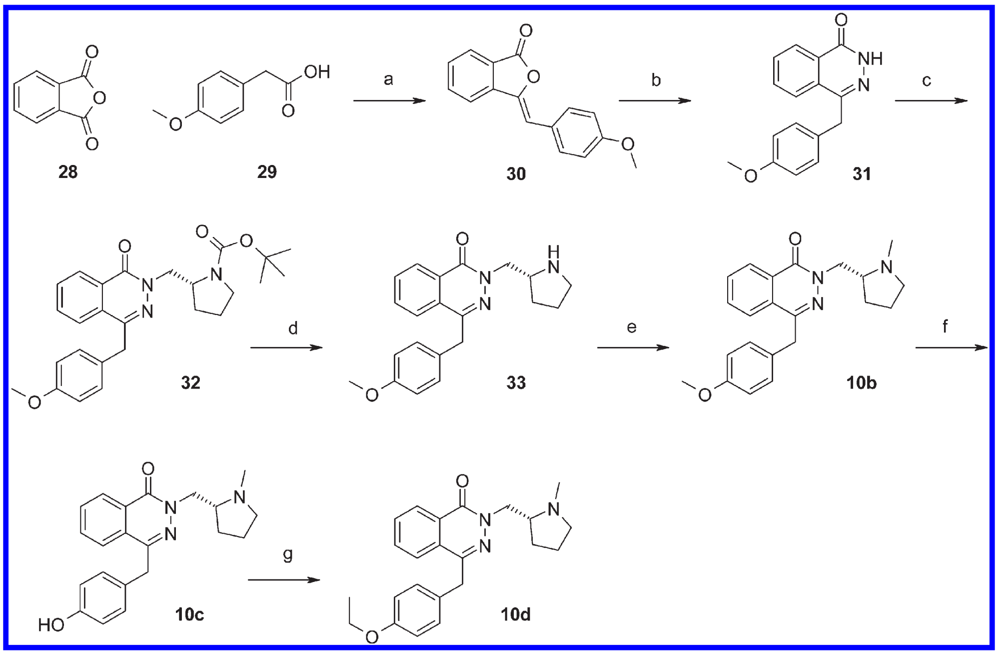

[a] Reagents and conditions: (a) NaOAc, 240 °C, 75%; (b) hydrazine sulfate, NaOH, EtOH, 95 °C, 91%; (c) *N*-Boc-D-prolinol, $PPh_3$, di-*tert*-butyl azodicarboxylate, THF, 91%; (d) TFA, DCM, 100%; (e) HCHO, $HCO_2H$, 95 °C, 80%; (f) $BBr_3$, DCM, 5 °C, 88%; (g) EtOH, $PPh_3$, di-*tert*-butyl azodicarboxylate, THF, 20 °C, 40%.

Scheme 7[a]

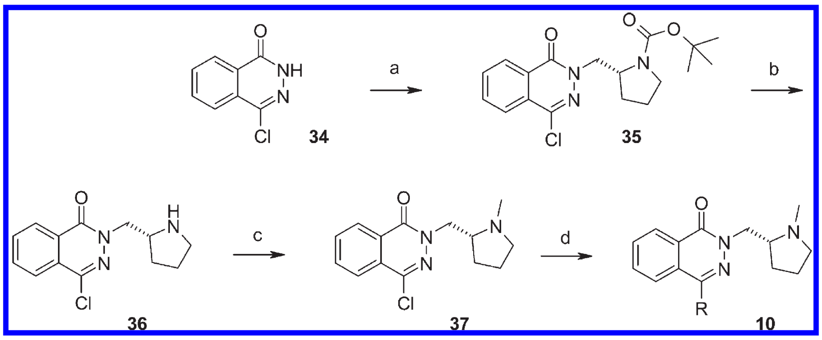

[a] Reagents and conditions: (a) *N*-Boc-D-prolinol, $PPh_3$, di-*tert*-butyl azodicarboxylate, THF, 100%; (b) 4 M HCl in dioxane, 66%; (c) HCHO, $HCO_2H$, 80 °C, 82%; (d) organozinc chloride or bromide, Pd[$(PPh_3)$]$_4$, THF, 80 °C.

the Trp residue in TM6 implied in the 7TM agonist state.[40] The edge of the phthalazinone core phenyl ring coordinated to the backbone of TM5. The effect of larger groups between the phthalazinone N2 group and the basic group was to push the phthalazinone nucleus onto the backbone of TM5, however, the combination of a flexible linker and a smaller heterocycle in the pyrrolidinomethyl analogues, relative to the azepine in azelastine, allowed for the phthalazinone moiety to adopt an orientation almost identical to that of azelastine (Figure 1).

The regioisomer **20** of azelastine had lower $H_1$ affinity than azelastine, and this is presumed to be due to its rigid structure, which after binding of the basic nitrogen to Asp-107 forces the phthalazinone core in an unfavorable orientation. Because the *R* enantiomer of the 2-pyrrolidinomethyl analogue (**10a**) had the highest $H_1$ affinity (9.8), this analogue was chosen for the optimization of the phthalazinone C4 substituent. Preferred substituents at C4 were found to be the 4-chloro- (**10a**), 4-methoxy- (**10b**), 4-hydroxy- (**10c**), 4-methyl- (**10f**), and 4-fluoro-benzyl (**10e**) analogues. Bulky substituents at the *para*-position of the C4-benzyl substituent, such as *tert*-butyl- (**10g**), methyl ester (**10h**), ethyl ether (**10d**), and ionic groups, such as carboxylic acid (**10i**), were not well tolerated. Alkyl substituents, such as cyclohexylmethyl (**10p**), phenethyl (**10q**), and pentyl (**10r**) had affinities much lower than that of a substituted benzyl group. The *meta*-substituted benzyl analogues of the highest affinity antagonists, such as the chloro- (**10k**), methyl- (**10m**), and methoxy- (**10l**), had lower affinity than the corresponding *para* analogues, whereas the *meta*-fluoro (**10j**) analogue had only slightly lower affinity. Two 3,4-disubstituted analogues were prepared, of which the dimethoxy analogue (**10o**) showed much reduced affinity, whereas the 3,4-difluoro analogue (**10n**) had affinity similar to that of the 4-fluoro analogue (**10e**), indicating that there is only limited space available in the pocket in which the benzyl substituent

**Table 2. Antagonist Affinity[a] of Target Compounds at the Human $H_1$ Receptor (Determined by Fluorescence Imaging Plate Reader), Human $H_3$ Receptor (Determined by a Functional GTP$\gamma$[S]-Assay), and Affinity at the Human $\alpha_{1A}$, and $\alpha_{1B}$ Receptors**

| compd | $H_1$ p$K_i$ (n) | $H_3$ p$K_i$ (n) | $\alpha_{1A}$ p$K_i$ (n) | $\alpha_{1B}$ p$K_i$ (n) |
|---|---|---|---|---|
| azelastine | 8.9 ± 0.0 (364) | 6.8 ± 0.0 (56) | 7.3 ± 0.0 (145) | 7.3 ± 0.0 (97) |
| **5** | 9.6 ± 0.1 (8) | <6.3 (7) | 6.8 ± 0.2 (3) | 6.7 ± 0.0 (3) |
| **6** | 8.0 ± 0.1 (6) | 6.9 ± 0.1 (4) | 6.5 ± 0.1 (3) | 6.5 ± 0.1 (3) |
| **10a** | 9.8 ± 0.1 (10) | 6.4 ± 0.0 (2) | 7.6 ± 0.1 (12) | 7.9 ± 0.2 (9) |
| **10b** | 10.0 ± 0.0 (8) | 7.1 ± 0.0 (2) | 6.9 ± 0.1 (4) | 6.8 ± 0.2 (4) |
| **10c** | 9.8 ± 0.1 (8) | 6.6 ± 0.1 (4) | 6.6 ± 0.2 (3) | 6.4 ± 0.1 (3) |
| **10d** | 8.3 ± 0.2 (6) | 6.5 ± 0.2 (2) | 6.1 (1) | <5.7 (3) |
| **10e** | 9.5 ± 0.1 (10) | <6.3 (8) | 7.2 ± 0.2 (4) | 7.1 ± 0.2 (4) |
| **10f** | 9.7 ± 0.1 (4) | <6.2 (5) | 8.0 ± 0.3 (3) | 7.8 ± 0.1 (3) |
| **10g** | 6.4 ± 0.0 (6) | <6.2 (6) | <5.7 (3) | <5.7 (3) |
| **10h** | 6.2 ± 0.1 (6) | <6.2 (4) | <5.7 (2) | <5.7 (3) |
| **10i** | <5.8 (6) | <6.2 (6) | <5.7 (3) | <5.7 (3) |
| **10j** | 9.3 ± 0.0 (6) | 6.7 ± 0.0 (6) | 7.3 ± 0.3 (4) | 6.4 ± 0.1 (4) |
| **10k** | 8.8 ± 0.1 (6) | <6.2 (5) | 6.4 ± 0.2 (5) | 6.2 ± 0.3 (2) |
| **10l** | 8.7 ± 0.1 (7) | 6.2 (1) | 5.8 ± 0.1 (2) | <5.7 (4) |
| **10m** | 9.1 ± 0.0 (6) | 6.6 ± 0.1 (5) | 6.3 ± 0.1 (3) | 6.3 ± 0.1 (3) |
| **10n** | 9.6 ± 0.1 (6) | <6.2 (6) | 6.7 ± 0.1 (3) | 6.5 ± 0.1 (3) |
| **10o** | 5.8 ± 0.0 (3) | <6.2 (10) | <5.7 (5) | <5.7 (5) |
| **10p** | 7.1 ± 0.0 (6) | 6.7 (1) | <5.7 (3) | <5.7 (3) |
| **10q** | 7.5 ± 0.0 (2) | <5.5 (2) | 6.7 (1) | 6.7 (1) |
| **10r** | 8.8 ± 0.1 (20) | <6.2 (6) | 6.3 ± 0.1 (3) | 6.0 ± 0.1 (2) |
| **11** | 9.5 ± 0.1 (10) | <6.4 (6) | 7.4 ± 0.2 (10) | 7.7 ± 0.2 (9) |
| **16** | 8.2 ± 0.1 (8) | <6.4 (8) | 7.0 ± 0.1 (6) | 7.1 ± 0.1 (6) |
| **18** | 9.0 ± 0.2 (10) | 6.9 ± 0.1 (7) | 7.8 ± 0.1 (6) | 8.2 ± 0.3 (6) |
| **19** | 7.2 ± 0.1 (18) | 7.1 ± 0.2 (5) | 6.5 ± 0.1 (5) | 6.5 (1) |
| **20** | 8.6 ± 0.0 (4) | <6.2 (4) | 6.8 ± 0.2 (2) | 6.8 ± 0.1 (2) |
| **38** | 7.3 ± 0.1 (8) | 9.3 ± 0.1 (8) | 7.0 ± 0.1 (10) | 6.9 ± 0.1 (7) |
| **39** | 7.8 ± 0.1 (6) | 8.4 ± 0.1 (2) | 7.5 ± 0.1 (3) | 7.5 ± 0.2 (3) |
| **40** | 7.8 ± 0.1 (4) | 9.6 ± 0.1 (4) | 6.9 ± 0.2 (2) | 7.1 ± 0.1 (2) |
| **41** | 7.7 ± 0.1 (13) | 8.7 ± 0.2 (8) | 6.8 ± 0.1 (10) | 7.0 ± 0.1 (8) |
| **54** | 7.4 ± 0.0 (6) | 9.4 ± 0.1 (6) | 6.5 ± 0.1 (4) | 6.5 ± 0.2 (3) |
| **55** | 7.4 ± 0.1 (4) | 8.1 ± 0.1 (4) | 5.8 (1) | <5.7 (2) |
| **56a** | 8.0 ± 0.1 (36) | 9.6 ± 0.0 (33) | 7.4 ± 0.0 (17) | 7.5 ± 0.1 (14) |
| **56b** | 8.1 ± 0.1 (8) | 9.5 ± 0.0 (8) | 7.2 ± 0.1 (5) | 7.3 ± 0.1 (5) |
| **56c** | 7.9 ± 0.1 (8) | 9.4 ± 0.1 (6) | 7.0 ± 0.0 (3) | 6.9 ± 0.0 (3) |
| **57** | 7.9 ± 0.1 (6) | 9.4 ± 0.0 (6) | 7.6 ± 0.2 (3) | 7.3 ± 0.1 (4) |
| **58** | 7.6 ± 0.1 (6) | 9.6 ± 0.1 (6) | 7.5 ± 0.2 (3) | 7.4 ± 0.0 (3) |

[a] Mean ± SEM (where applicable) of estimated functional p$K_i$. For $n < 3$ SEM is the SD. n = number of experiments.

binds. The highest affinity analogues **10a**−**c**, **10e**, and **10f** were also found to be selective for $H_1$ against $H_3$, $\alpha_{1A}$ and $\alpha_{1B}$, however, **10f** had reduced selectivity against $\alpha_{1A}$ and $\alpha_{1B}$.

## 3. DUAL $H_1H_3$ ANTAGONISM

Having established the optimal C4 and N2 phthalazinone substituents for maximal antagonism at the human $H_1$ receptor, attention was focused on identifying dual human $H_1H_3$ antagonism in a single ligand. Examination of the $H_1$ homology model indicated the existence of a narrow channel between TM2, TM3, TM6, and TM7, extending parallel to the helix axes deeper into the 7TM bundle, which may be reached from the basic center of azelastine (Figure 1). From our preliminary investigations with azelastine analogues, it was found that high $H_1$ antagonism was retained with a large number of substituents on its basic nitrogen. It was envisioned that introduction of fragments associated with $H_3$ antagonism, such as a phenoxypropylamino group, would bring about dual $H_1H_3$ antagonism (Chart 3).

It was necessary to investigate first the optimal chain-length of the linker group between azelastine's basic nitrogen and the point

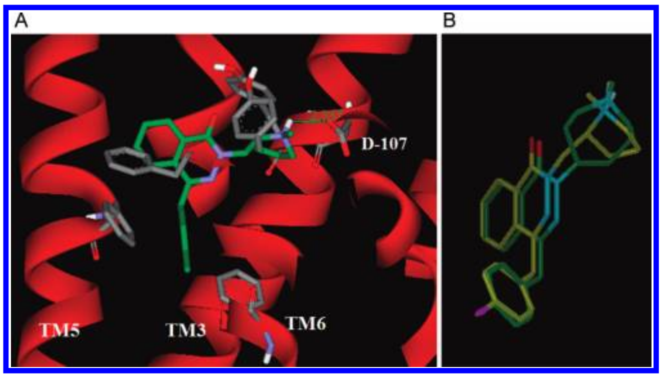


**Figure 1.** (A) One of the low energy conformations of azelastine docked into the homology model of H1. (B) Overlay of the docked poses of azelastine (green) and **11a**.

**Chart 3. Strategy for Dual $H_1$ $H_3$ Antagonism on a Single Ligand**

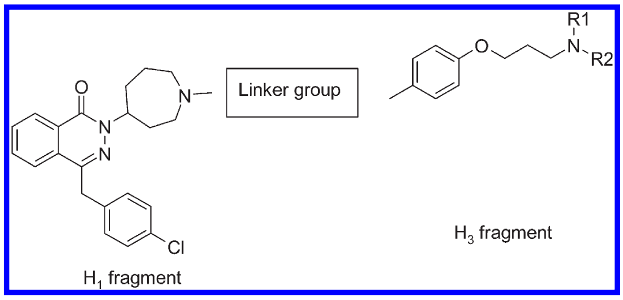


of attachment of the $H_3$ fragment. Furthermore, our early investigations with a nonphthalazinone $H_1$ fragment indicated that the human $H_1$ antagonism of dual $H_1H_3$ antagonists was found to be very sensitive to the amino group of the $H_3$ fragment. For this reason, the homopiperidinopropyloxyphenyl group, which was found to be one of the higher affinity $H_3$ fragments in our ketopiperazine selective $H_3$ antagonists,[29] was chosen for attachment onto the basic nitrogen of the optimized $H_1$ phthalazinones **10a**−**c** and **5** identified above.

**3.1. Chemistry.** A series of azelastine derivatives **38**−**41**[41] incorporating a linker group consisting of one to four methylenes to the $H_3$ fragment was prepared by alkylation of des-methyl azelastine (**42**) and an appropriate electrophile, such as **43** (Chart 4). The mesylate **43** was prepared by the method outlined in Scheme 8. Thus, reaction of 4-iodophenol (**45**) with 1-bromo-3-chloropropane gave chloride **46**, which was treated with hexamethyleneimine to provide amine **47**. Sonogashira coupling of **47** with 3-butyn-1-ol yielded **48**, which was converted to the alcohol **49** by catalytic hydrogenation and then treated with methanesulfonyl chloride to give the mesylate **43**.

The homologue of **43**, mesylate **44**, was prepared by the method outlined in Scheme 9. Thus, Mitsunobu alkylation of phenol **50**[42] with alcohol **51**[43] provided **52**, which was reduced with lithium aluminum hydride to give alcohol **53** and, in turn, converted to mesylate **44**. Alkylating agents **43** and **44** were found to deteriorate with time at room temperature, so they were stored at −20 °C or made freshly before use.

Alkylation of **4** with mesylate **43** gave **54**, which was then converted to the tertiary amine **55** by Eschweiler−Clarke alkylation (Scheme 10).

Chart 4. Variation of the Linking Group between the $H_1$ and $H_3$ Fragments [a]

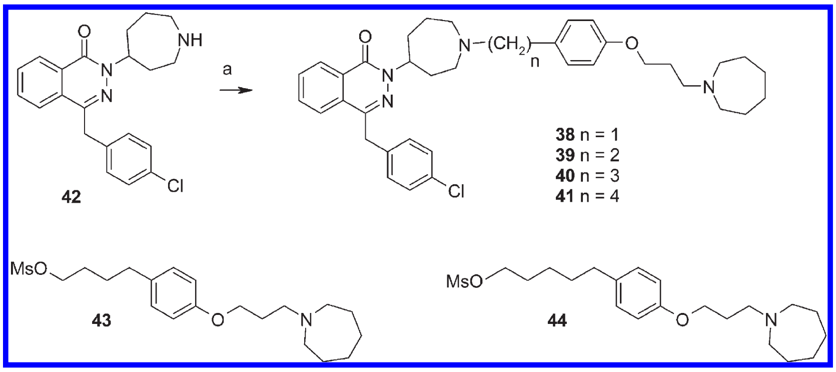


[a]Reagents and conditions: (a) Alkyl mesylate, $NaHCO_3$, MeCN, reflux.

Scheme 8[a]

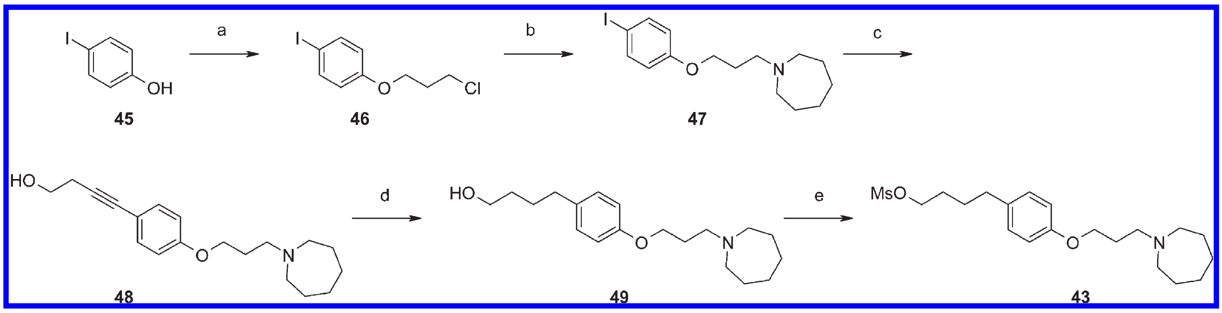


[a] Reagents and conditions: (a) 1-bromo-3-chloropropane, $K_2CO_3$, 2-butanone, reflux, 84%; (b) hexamethyleneimine, NaI, 2-butanone, 80 °C, 83%; (c) 3-butyn-1-ol, $Et_3N$, $(PPh_3)_2PdCl_2$, CuI, THF, 20 °C, 77%; (d) $H_2$, 10% Pd/C, HCl, EtOH, MeOH, 88%; (e) MsCl, $iPr_2NEt$, DCM, 20 °C, 94%.

Scheme 9[a]

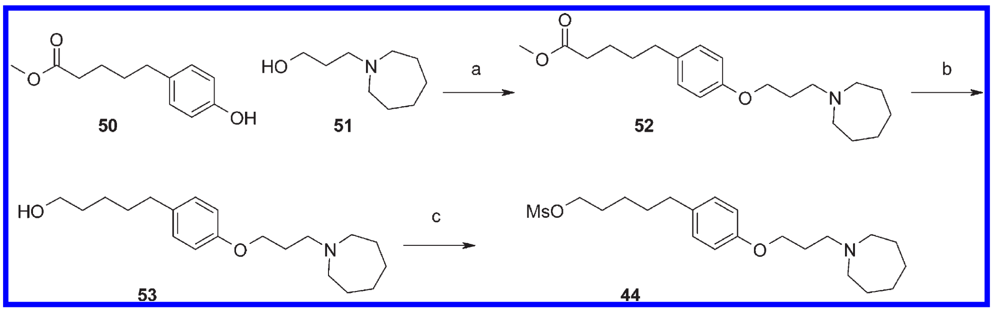


[a] Reagents and conditions: (a) $PPh_3$, di-*tert*-butyl azodicaroxylate, THF, 69%; (b) $LiAlH_4$, THF, 68%; (c) MsCl, $iPr_2NEt$, DCM, 20 °C, 100%.

The chloro- and methoxy- analogues (**56a** and **56b**, respectively) were prepared by alkylation of the appropriate amine (**14** and **33**, respectively) with the mesylate **43**, whereas the hydroxy- analogue (**56c**) was prepared from **56b** by treatment with boron tribromide. The homologue of **56a** (**57**) was prepared by reacting **14** with mesylate **44** (Scheme 11).

A second, nonconvergent route was used for the synthesis of **56a** and its enantiomer **58**. This route, outlined in Scheme 12, was not suitable for array chemistry, however, it was more suitable for larger scale work. All the intermediates in this route (**59**−**63**) were either neutral or monobasic compounds and therefore more readily purified by chromatography than dibasic compounds.

**3.2. Results and Discussion.** The first dibasic, bivalent ligands to be tested were the analogues bearing the azelastine $H_1$ azepine group linked to the $H_3$ fragment with an alkyl-chain linker of one to four methylenes (compounds **38**−**41**) in order to determine the chain-length requirement for the linker. In the $H_1$ homology model, the $H_3$ fragment of the bivalent ligands could be threaded into a narrow channel between TM2, TM3, TM6, and TM7. While the longer-chain analogues fit well into the available space, molecule **38** additionally formed an H-bond with the Asp-73 side chain in TM2 (Figure 2). The compounds were not docked into the $H_3$ homology model where this narrow channel also existed, albeit with a different shape. The qualitative modeling results were confirmed by the low nanomolar affinity of **38**−**41** at the $H_3$ receptor and high nanomolar affinity at $H_1$. However, the shorter-chain analogue (**38**) was less active than the longer analogues, which means that the additional H bond to Asp-73

Scheme 10[a]

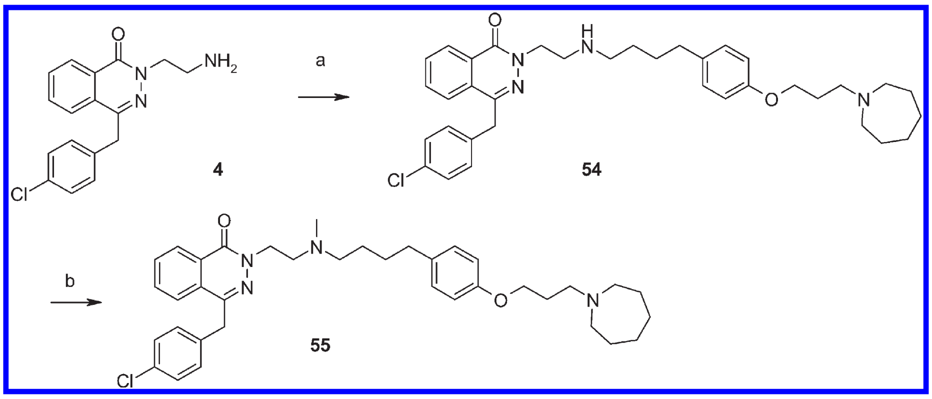


[a] Reagents and conditions: (a) **43**, $NaHCO_3$, MeCN, reflux, 21%; (b) HCHO, $HCO_2H$, 100 °C, 66%.

Scheme 11[a]

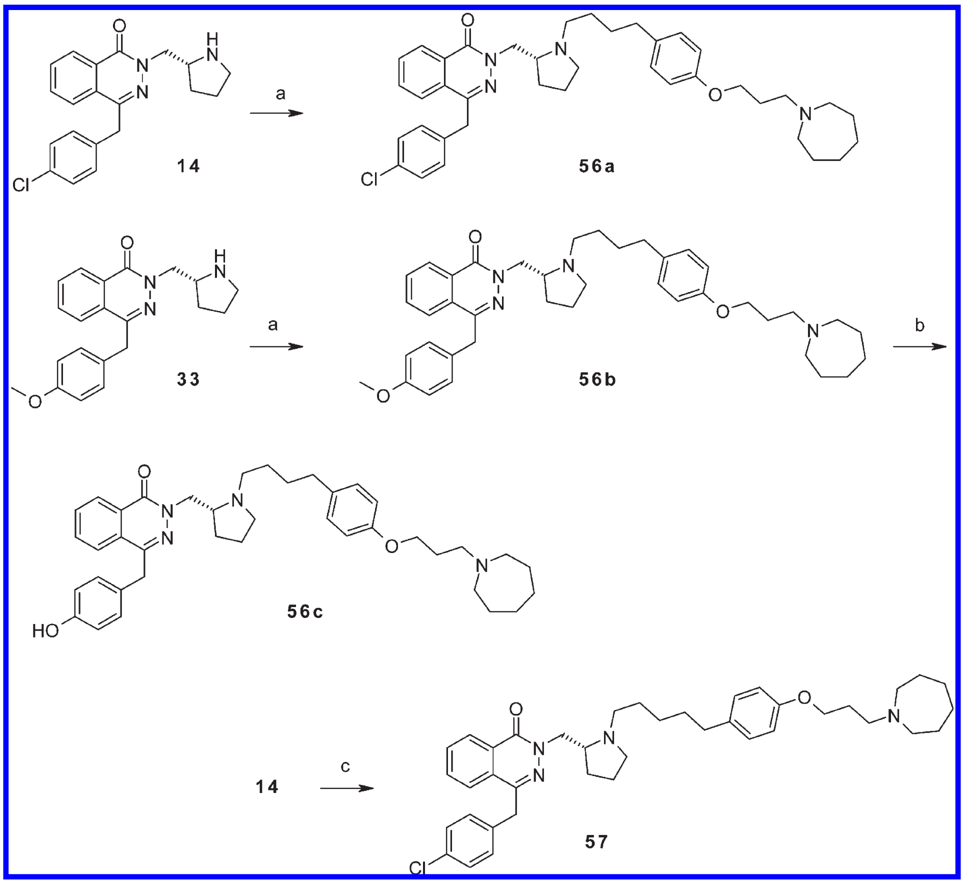


[a] Reagents and conditions: (a) **43**, $NaHCO_3$, MeCN, reflux, 35%; (b) $BBr_3$, DCM, 5 °C, 14%; (c) **44**, $NaHCO_3$, MeCN, reflux, 21%.

was either not formed or the $H_1$ homology model did not reflect the observed SAR.

Compounds **38** and **40** were more potent at $H_3$ (about 100-fold) and were not progressed; the data is shown in Table 2. Compounds **39** and **41** had a more acceptable difference of about 10-fold, however, **41** was more selective than **39** for $H_1$ over $\alpha_{1A}$ and $\alpha_{1B}$, hence the four methyl linker was chosen for optimizing the $H_1$ fragment. Analogues **54** and **55**, bearing flexible chain linkers, had greatly reduced $H_1$ affinity by comparison to the monovalent ligand **5** (Table 2) and were therefore not progressed. The analogues **56a**−**c** and **57** had high $H_3$-receptor affinity (p$K_i$ values between 9.4 and 9.6), which is almost 3 orders of magnitude greater than azelastine ($H_3$ p$K_i$ 6.8). However, their $H_1$-receptor functional p$K_i$ values were about 8, which represented a drop of 2 orders of magnitude by comparison with their monovalent analogues. Despite the reduction in $H_1$-receptor affinity, compounds **56a**−**c** and **57** are to our knowledge among the most potent bivalent $H_1H_3$ antagonists known.[28] The *R*-enantiomer **56a** had greater $H_1$ affinity than the *S*-isomer **58**, as was the case with the monovalent analogues (cf **10a** with **11**).

Scheme 12[a]

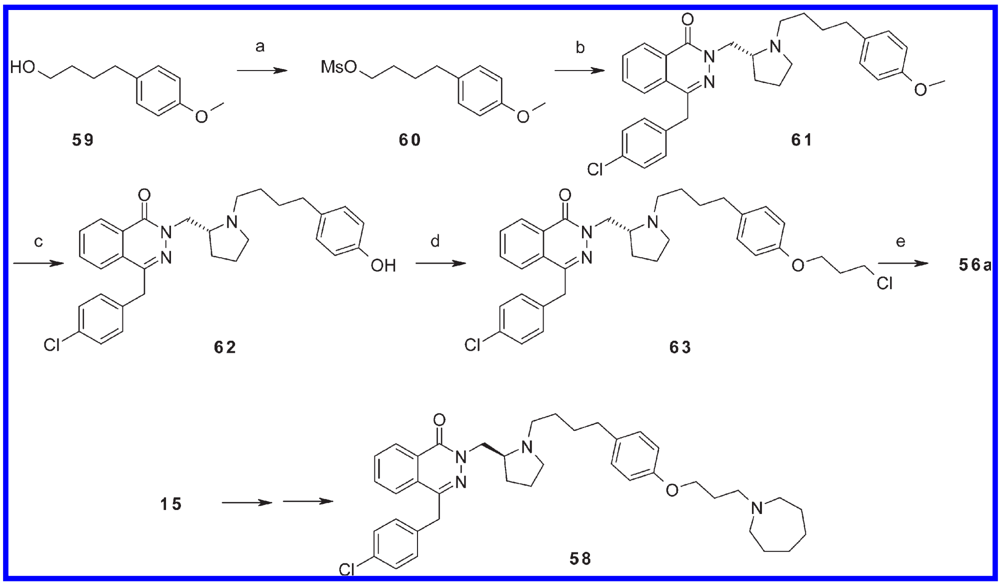


[a] Reagents and conditions: (a) MsCl, $Et_3N$, $Et_2O$, 0 °C, 100%; (b) **14**, $K_2CO_3$, 2-butanone, reflux, 24 h, 60%; (c) $BBr_3$, DCM, −60 °C, 93%; (d) 1-bromo-3-chloropropane, $K_2CO_3$, 2-butanone, reflux, 18 h, 85%; (e) hexamethyleneimine, KI, $K_2CO_3$, 2-butanone, reflux, 41 h, 48%.

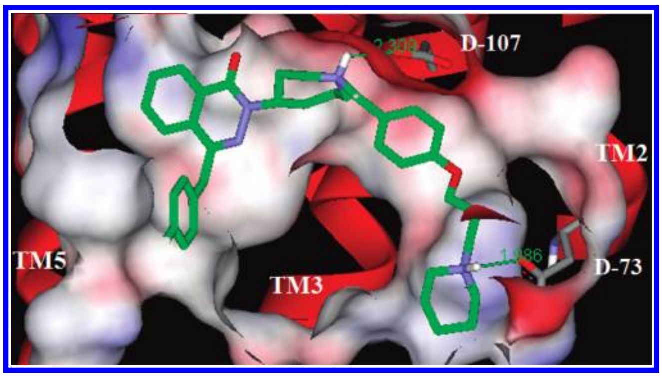


**Figure 2.** One of the low-energy conformations of the extended azelastine ligand **40** docked into the homology model of $H_1$.

In addition to the assays reported in Section 2.2, a more precise, lower throughput, modified version of the human $H_1$ FLIPR assay was run, which provided apparent $pA_2$ values. Antagonist $pA_2$ values were determined by generating histamine concentration−response curves either in the absence or presence of a single concentration of antagonist (100 nM) at 30 min incubation. The histamine concentration−response curves were analyzed using a four-parameter logistic equation to determine the midpoint ($EC_{50}$) of the curve. Antagonist $pA_2$ values were calculated using the equation $pA_2 = \log(DR - 1) - \log[B]$ where DR, the dose ratio, is the $EC_{50}$ in the presence of antagonist divided by the $EC_{50}$ for the control curve, and [B] is the molar concentration of the antagonist tested. The data for dual antagonists **56a−c** and **57** are summarized in Table 3 and compared to azelastine. Compound **56a** was the most potent $H_1$ antagonist ($pA_2$ 9.1). Duration of action in vitro was determined in the FLIPR assay by incubation of adherent CHO cells with antagonist for 30 min, followed by washing, and then by repeat histamine challenges at intervals of 90 and 270 min at 37 °C. Agonist dose ratios were converted to receptor occupancies, which were plotted against time. A measure of duration was obtained from the gradient of the percent receptor occupancy versus time plot. Results were statistically analyzed and related to azelastine in the same assay and expressed as slower, no-difference, or faster wash-out than azelastine, with slower wash-out equating to longer duration of action. Duration of action for bivalent antagonists **56a−c** and **57** is summarized Table 3. Antagonists **56a−c** were all found to be longer-acting than azelastine, however, **57** had the same duration as azelastine.

**Table 3. Antagonist $pA_2$ Affinity of 56a−c and 57 at the Human $H_1$ Receptor, Determined by Fluorescence Imaging Plate Reader and in Vitro Duration**

| compd | $pA_2 \pm$ SEM[a] | *n* | wash-out |
|---|---|---|---|
| **56a** | 9.1 ± 0.1 | 11 | slower |
| **56b** | 8.9 ± 0.1 | 10 | slower |
| **56c** | 8.4 ± 0.1 | 8 | slower |
| **57** | 8.9 ± 0.1 | 6 | no difference |
| azelastine | 9.7 ± 0.1 | 19 | reference |

[a] All $pA_2$ values taken from curve shifts generated at 30 min incubation time and with 100 nM antagonist.

The specificity profile of compounds **56a** and **56b** was evaluated by comparison to that of the clinical gold-standard, azelastine, and all three compounds were found to have a similar profile against $\alpha_{1A}$ and $\alpha_{1B}$ (Table 2). In addition, **56a** had low affinity for the human $H_2$ and $H_4$ receptors ($pIC_{50}$ 5.0). However, **56a** showed significant affinity ($pIC_{50}$ 7.3) for the hERG channel, having a very similar affinity to azelastine ($pIC_{50}$ 7.0) in the hERG dofetilide binding assay. Further assessment of the hERG effects of **56a** in an electrophysiology patch clamp confirmed the dofetilide displacement data. However, subsequent evaluation in rabbit hearts in vitro (SCREENIT model) suggested that the risk of **56a**-induced QT prolongation is low at therapeutically relevant concentrations.

The in vitro rate of metabolism of **56a** in human liver microsomes was moderate; the rate in human hepatocytes, however, was low. The rate of in vitro hepatic metabolism was generally

Table 4. In Vivo Pharmacokinetic Profile of 56a and Azelastine in Male CD Rats and Male Beagle Dogs

| compound dose (mg/kg) (route) | species | Cl (mL/min/kg) [range] % LBF | $V_{ss}$ (L/kg) [range] | $t_{1/2}$ (h) [range] | F (%) [range] |
|---|---|---|---|---|---|
| **56a** 3.0 (po)/1.0 (iv) | rat (*n* = 7) | 30 [16–49] 35% | 3.9 [2.0–4.6] | 2.2 [1.6–3.5] | 4 [1–10] |
| **56a** 3.0 (po)/1.0 (iv) | dog (*n* = 3) | 27 [23–34] 87% | 22 [5.9–51] | 9.4 [3.4–20] | 19 [17–23] |
| azelastine 3.0 (po)/1.0 (iv) | rat (*n* = 3) | 35 [28–40] 41% | 1.8 [1.6–2.1] | 1.0 [1.0–1.1] | 7 [7–7] |
| azelastine 2.0 (po)/1.0 (iv) | dog (*n* = 1) | 22 | 4.9 | 3.2 | 46 |

moderate for rat and dog and was in agreement with its clearance obtained in vivo. The pharmacokinetic profile of compound **56a** was evaluated in rat and dog and summarized in Table 4. In the male CD rat, **56a** had moderate in vivo clearance, and in the male Beagle dog, the clearance was high (35% and 87% of liver blood flow, respectively). Over a 24 h period, excretion of unchanged **56a** in dog urine was <1% following both oral and intravenous administration, suggesting that elimination via renal clearance was low. The steady state volume of distribution ($V_{ss}$) for **56a** was moderate for the rat and high for the dog (3.9 and 22 L/kg, respectively). However, there was significant variability in the estimatation of $V_{ss}$ for the dog. After intravenous administration, **56a** had a moderate blood half-life in the rat and a long blood half-life in the dog (2.2 and 9.4 h, respectively). In the dog, the long half-life is volume driven and significant variability was observed in line with the variability observed with $V_{ss}$. Systemic exposure following oral administration of **56a** was very low in the rat (4%) and higher in the dog (19%). Following oral administration of **56a**, low concentrations of the compound were detected in blood sampled from the hepatic portal vein (1–6% of the dose) due to either low absorption and/or high first-pass metabolism. The bioavailability of azelastine in humans following intranasal administration was reported to be 40%.[13] The rat and dog pharmacokinetic parameters for azelastine are included in Table 4 and clearly show that **56a** had twice as long as azelastine's half-life and that the oral bioavailability of **56a** was lower than that of azelastine's in both species.

To avoid sedation, it is necessary to have a low brain concentration of $H_1$ receptor antagonist following an intranasal therapeutic dose. Azelastine gave a brain–blood ratio of 7.5 (range 6.2–8.6) following intravenous infusion to the male CD rat. However, **56a** gave a brain–blood ratio of 0.6 (range 0.3–1.1). Therefore, the risk of engaging CNS related side-effects associated with either $H_1$ or $H_3$ would be very low considering the clinical dose and the low bioavailability of **56a**.

Several second-generation $H_1$ antagonists are substrates and modulators of hepatic cytochrome P450, in particular the subtype CYP3A4. Azelastine inhibits mainly CYP2D6 ($IC_{50}$ 1 $\mu$M). For compounds designed for oral dosing, it is essential to avoid any drug–drug interactions that might lead to CYP450 activation and reduced safety in the clinic. **56a** showed an acceptable in vitro inhibition profile against CYP1A2, CYP2C9, and CYP2C19 ($IC_{50}$ >3 $\mu$M), however, it was found to be a potent inhibitor of CYP2D6 ($IC_{50}$ 0.04 $\mu$M) and CYP3A4 ($IC_{50}$ 0.3 $\mu$M). As its oral bioavailability is low, and the intended clinical intranasal dose is predicted to be low, coadministration with **56a** is unlikely to result in significant clinical drug–drug interactions. Furthermore, there was no evidence of time-dependent P450 inhibition for the CYP3A4 and CYP2D6 isoforms.

In vivo pharmacology of **56a** and azelastine was studied in conscious guinea pigs in which nasal congestion was induced by intranasal histamine instillation and measured indirectly by plethysmography. Compound **56a** dosed by intranasal instillation of 0.1 and 1 mg/mL antagonized the histamine induced response with a duration of up to 72 h, whereas azelastine antagonized the response with a duration of <24 h at 1 mg/mL. These data are consistent with potential clinical application of a once a day intranasal treatment for allergic rhinitis. Further pharmacological findings, such as the time-dependent increase in the binding affinity of **56a** and the in vivo inhibition of histamine-induced nasal airway resistance in guinea pigs, will be published elsewhere.[44]

Various salts of **56a** were prepared, and two of these are noteworthy: the dihydrochloride and the 1,5-naphthalene disulfonate salts. The former was a highly soluble salt (>11 mg/mL in PBS at pH 5) and log *D* 2.86, whereas the latter was a crystalline salt with low solubility (20 $\mu$g/mL) and log *D* 3.0. For comparison, the solubility of azelastine hydrochloride salt was 144 $\mu$g/mL in PBS (pH 7.4) and its log *D* 2.25.

## 4. CONCLUSION

A series of potent phthalazinone-based human $H_1H_3$ bivalent human histamine receptor antagonists were synthesized. Compounds **56a** and **56b** had $H_1$ potency slightly lower than that of the clinical gold-standard, azelastine, and $H_3$ potency nearly 3 orders of magnitude greater than that of azelastine. In addition, **56a** and **56b** had longer duration of action in vitro on histamine-induced stimulation of human recombinant $H_1$ receptors than azelastine. Furthermore, following intranasal dosing, **56a** is a potent inhibitor of histamine-induced nasal airway resistance in guinea pigs in vivo, with significantly longer duration of action than that of azelastine and efficacy at a 10 times lower concentration. The in vivo pharmacokinetic characteristics of **56a** were indicative of limited systemic exposure from the swallowed portion of an intranasal dose, which should limit the potential for unwanted side effects. Brain penetration from iv dosing in the rat was lower than azelastine's, which coupled with the low clinical dose and low bioavailability, should limit the potential for engaging CNS related side effects associated with either $H_1$ or $H_3$ antagonism. CYP2D6 and CYP3A4 were inhibited by **56a**, however, as both the intended clinical dose and oral bioavailability are predicted to be low, coadministration with **56a** is unlikely to result in significant clinical drug–drug interactions. There was also no evidence of time-dependent P450 inhibition for either CYP3A4 or CYP2D6. On the basis of the above data, **56a** was chosen for further progression as an intranasal treatment for allergic rhinitis.

## 5. EXPERIMENTAL SECTION

Organic solutions were dried over anhydrous $Na_2SO_4$ or $MgSO_4$. TLC was performed on Merck 0.25 mm Kieselgel 60 $F_{254}$ plates. Products were visualized under UV light and/or by staining with aqueous $KMnO_4$ solution. LCMS analysis was conducted on a Supelcosil LCABZ+PLUS column (3.3 cm × 4.6 mm i.d.) eluting with 0.1% formic acid and 0.01 M ammonium acetate in water (solvent A) and 0.05% formic acid and 5% water in acetonitrile (solvent B), using the following elution gradient 0.0–0.7 min 0% B, 0.7–4.2 min 100% B, 4.2−5.3 min 0% B, 5.3−5.5 min 0% B at a flow rate of 3 mL $min^{-1}$. The mass spectra were recorded on a Fisons VG Platform spectrometer using electrospray positive and negative mode (ES+ve and ES−ve). Column chromatography was performed on Flashmaster II. The Flashmaster II is an automated multiuser flash chromatography system, available from Argonaut Technologies Ltd., which utilizes disposable, normal phase, SPE cartridges (2−100 g). Mass-directed autopreparative HPLC (MDAP) was conducted on a Waters FractionLynx system comprising a Waters 600 pump with extended pump heads, Waters 2700 autosampler, Waters 996 diode array, and Gilson 202 fraction collector on a 10 cm × 2.54 cm i.d. ABZ+ column, eluting with 0.1% formic acid in water (solvent A) and 0.1% formic acid in acetonitrile (solvent B), using an appropriate elution gradient over 15 min at a flow rate of 20 mL $min^{-1}$ and detecting at 200−320 nm at room temperature. Mass spectra were recorded on Micromass ZMD mass spectrometer using electrospray positive and negative mode, alternate scans. The software used was MassLynx 3.5 with OpenLynx and FractionLynx options. $^{1}$H NMR spectra were recorded at 400 MHz. The chemical shifts are expressed in ppm relative to tetramethylsilane. High resolution positive ion mass spectra were acquired on a Micromass Q-Tof 2 hybrid quadrupole time-of-flight mass spectrometer. Optical rotations were measured with an Optical Activity AA100 digital polarimeter. Analytical chiral HPLC was conducted on Chiralpak column (250 mm × 4.6 mm) eluting with 15% EtOH−heptane for 30 min at room temperature, flow rate 1 mL $min^{-1}$, injection volume 15 μL, detecting at 215 nm. The purity of all compounds screened in the biological assays was examined by LCMS analysis and was found to be ≥95%, unless otherwise specified. The purity of crystalline salts was additionally assessed by elemental microanalysis.

**4-[(4-Chlorophenyl)methyl]-2-{2-[[4-(4-{[3-(hexahydro-1*H*-azepin-1-yl)propyl]oxy}phenyl)butyl](methyl)amino]ethyl}-1(2*H*)-phthalazinone (55).** A suspension of 4-[(4-chlorophenyl)methyl]-2-(2-{[4-(4-{[3-(hexahydro-1*H*-azepin-1-yl)propyl]oxy}phenyl)butyl]amino}ethyl)-1(2*H*)-phthalazinone (**54**) (16 mg, 0.027 mmol) in formaldehyde (37 wt % in water, 2 mL) and formic acid (0.20 mL) was heated at 100 °C with stirring for 40 min. After cooling, the mixture was concentrated in vacuo. The residue was then heated on a steam bath, under high vacuum for 2 h, to give **55** (11 mg, 66%) without further purification: LCMS RT = 2.47 min, 95%, ES+ve *m*/*z* 615 $[M + H]^+$ and 308/309 $[M/2 + H]^+$. $^{1}$H NMR δ ($CD_3OD$) 8.37−8.33 (1H, m), 7.90−7.85 (1H, m), 7.84−7.76 (2H, m), 7.28 (2H, d, *J* = 8 Hz), 7.23 (2H, d, *J* = 8 Hz), 6.91 (2H, d, *J* = 8.5 Hz), 6.72 (2H, d, *J* = 8.5 Hz), 4.36 (2H, t, *J* = 6.5 Hz), 4.29 (2H, s), 3.94 (2H, t, *J* = 6 Hz), 2.85 (2H, t, *J* = 6.5 Hz), 2.83−2.73 (6H, m), 2.45−2.38 (4H, m), 2.30 (3H, s), 2.01−1.92 (2H, m), 1.76−1.60 (8H, m), 1.48−1.38 (4H, m). HRMS ES+ve *m*/*z*: calcd for $C_{37}H_{48}ClN_4O_2$, 615.3466; found, 615.3489.

**4-[(4-Chlorophenyl)methyl]-2-({(2*R*)-1-[4-(4-{[3-(hexahydro-1*H*-azepin-1-yl)propyl]oxy}phenyl)butyl]-2-pyrrolidinyl}methyl)-1(2*H*)-phthalazinone (56a) Free Base.** A mixture of **14** (1.017 g, 2.87 mmol), **43** (1.115 g, 2.91 mmol), and sodium bicarbonate (474 mg, 5.64 mmol) in MeCN (50 mL) was heated at 80 °C with stirring for 5 days under a nitrogen atmosphere. The cooled reaction mixture was partitioned between water and EtOAc. The aqueous layer was washed with further EtOAc (×2). The combined organic extracts were dried ($MgSO_4$) and concentrated in vacuo. The residue (1.35 g) was dissolved in DMF−TFA (2:1, 15 mL) and purified by preparative HPLC, using a Kromasil C8 column (28 cm × 5 cm), eluting with a gradient of 5−45% (MeCN containing 0.25% TFA)−(0.25% TFA in water) over 40 min, followed by holding the final solvent ratio for a further 15 min. The relevant fractions were combined and concentrated in vacuo to leave an aqueous solution. This was applied to an Amberchrom CG-161 M column (25 cm × 2.5 cm), and the column was washed with water to remove excess TFA and eluted with MeCN to afford the product as the trifluoroacetate salt. This was redissolved in MeCN and applied to a SCX cartridge (20 g), preconditioned with MeOH then MeCN, and eluting with MeCN, followed by a solution of 10% aqueous 0.88 ammonia in MeCN. The appropriate fractions were concentrated under reduced pressure to give **56a** (651 mg, 35%): LCMS RT = 2.52 min, ES+ve *m*/*z* 641 $[M + H]^+$ and 321/322 $[M/2 + H]^+$. $^{1}$H NMR (DMSO-$d_6$) δ 8.38 (1H, dd, *J* = 7.7, 1.6 Hz), 7.93 (1H, m), 7.86 (1H, m), 7.82 (1H, m), 7.30 (4H, m), 7.03 (2H, d, *J* = 8.5 Hz), 6.80 (2H, d, *J* = 8.5 Hz), 4.36 (1H, m), 4.33 (2H, s), 4.14 (1H, dd, *J* = 13.1, 8.0 Hz), 3.98 (2H, t, *J* = 6.1 Hz), 3.14 (1H, m), 3.03 (1H, dd, *J* = 7.8, 4.5 Hz), 2.84 (1H, m), 2.75 (6H, m), 2.50 (2H, t, *J* = 6.9 Hz), 2.31 (2H, m), 1.97 (2H, m), 1.82 (4H, m), 1.68 (8H, m), 1.55 (4H, m).

**4-[(4-Chlorophenyl)methyl]-2-({(2*R*)-1-[4-(4-{[3-(hexahydro-1*H*-azepin-1-yl)propyl]oxy}phenyl)butyl]-2-pyrrolidinyl}methyl)-1(2*H*)-phthalazinone, (56a)-1,5-Naphthalene Disulfonate Monohydrate Salt.** Free base **56a** (400 mg, 0.62 mmol) was dissolved in methanol (4.44 mL). A solution of 1,5-naphthalene disulfonic acid (232 mg, 0.80 mmol) in methanol (1 mL) was added, and the resulting gummy solution was heated. Small amounts of solid began to form, and on cooling a solid precipitated. The slurry was stirred at room temperature for approximately 1 h, and methanol (2 mL) was added to mobilize the slurry, which was heated and cooled again and left to stir for a further hour. The solid was isolated by filtration and dried in vacuo at 40 °C to give **56a**-1,5-naphthalenedisulfonate salt (465 mg, 73%): mp (DSC) 234−240 °C; $[\alpha]_D^{20}$ +8.0 (*c* 1.05 in DMSO). $^{1}$H NMR (DMSO-$d_6$) δ 9.10 (2H, br), 8.86 (2H, d, *J* = 9 Hz), 8.31 (1H, br d, *J* = 7 Hz), 8.00−7.84 (5H, m), 7.43−7.33 (6H, m), 7.07 (2H, d, *J* = 9 Hz), 6.82 (2H, m), 4.55 (2H, d, *J* = 5 Hz), 4.31 (2H, m), 3.96 (2H, t, *J* = 6 Hz), 3.85 (1H, m), 3.62 (1H, m), 3.53−3.27 (9H, m), 3.26−3.19 (2H, m), 3.19−3.03 (4H, m), 2.22−1.43 (18H, m). Found: C, 61.8; H, 6.2; N, 5.8; S, 6.8; Cl, 3.6. $C_{39}H_{49}ClN_4O_2 \cdot C_{10}H_8O_6S_2$ requires C, 62.1; H, 6.3; N, 5.9; S, 6.8; Cl, 3.7%

**4-[(4-Chlorophenyl)methyl]-2-({(2*R*)-1-[4-(4-{[3-(hexahydro-1*H*-azepin-1-yl)propyl] oxy}phenyl)butyl]-2-pyrrolidinyl}methyl)-1(2*H*)-phthalazinone, (56a)-Dihydrochloride.** Free base **56a** (3.85 g, 6.0 mmol) was dissolved in MeOH (100 mL), and 2 M hydrochloric acid (12 mL, 24 mmol) was added. The solution was then evaporated under reduced pressure, and the residue was dissolved in MeOH (50 mL) and re-evaporated. The addition of MeOH and evaporation was repeated three times, and the residue was dried in vacuo to give **56a**·2HCl (4.3 g, 100%). $^{1}$H NMR (DMSO-$d_6$) δ 10.60 (1H, br s), 10.49 (1H, br s), 8.30 (1H, dd, *J* = 7.5, 1.5 Hz), 7.96 (1H, d, *J* = 7.5 Hz), 7.93−7.88 (1H, m), 7.89−7.84 (1H, m), 7.38 (2H, d, *J* = 8.5 Hz), 7.34 (2H, d, *J* = 8.5 Hz), 7.09 (2H, d, *J* = 8.5 Hz), 6.84 (2H, d, *J* = 8.5 Hz), 4.62 (1H, dd, *J* = 14, 4.5 Hz), 4.55 (1H, dd, *J* = 14, 7 Hz), 4.37 (1H, d, *J* = 16.5 Hz), 4.33 (1H, d, *J* = 16.5 Hz), 4.00 (2H, t, *J* = 6 Hz), 3.85−3.77 (1H, m), 3.64−3.55 (1H, m), 3.46−3.31 (3H, m), 3.22−3.15 (2H, m), 3.14−3.02 (4H, m), 2.53−2.47 (2H, m), 2.23−2.07 (4H, m), 1.99−1.49 (14H, m).

**2-({(2*R*)-1-[4-(4-{[3-(Hexahydro-1*H*-azepin-1-yl)propyl]oxy}phenyl)butyl]-2-pyrrolidinyl}methyl)-4-{[4-(methyloxy)phenyl]methyl}-1(2*H*)-phthalazinone (56b) diformate.** Was prepared by a procedure similar to that described for **56a** substituting **14** with **33** LCMS RT = 2.37 min, 95%, ES+ve *m*/*z* 637 $(M + H)^+$, 319 $(M/2 + H)^+$. $^{1}$H NMR δ ($CD_3OD$) 8.48 (2H, br s), 8.40−8.35 (1H, m), 7.98 (1H, m), 7.90−7.80 (2H, m), 7.22 (2H, d, *J* = 9 Hz), 7.06 (2H, d, *J* = 9 Hz), 6.86−6.80 (4H, m), 4.58 (2H, m), 4.28 (2H, s), 4.03 (2H, t, *J* = 6 Hz), 3.88−3.80 (1H, m), 3.72 (3H, s), 3.66−3.58 (1H, m), 3.40−3.32 (5H, m), 3.11−2.95 (2H, m), 2.53 (2H, t, *J* = 7 Hz), 2.30−2.16 (4H, m), 2.11−1.88 (8H, m), 1.78−1.57 (8H, m). HRMS ES+ve *m*/*z*: calcd for $C_{40}H_{53}N_4O_3$, 637.4118; found, 637.4125

**2-({(2*R*)-1-[4-(4-{[3-(Hexahydro-1*H*-azepin-1-yl)propyl]oxy}phenyl)butyl]-2-pyrrolidinyl}methyl)-4-[(4-hydroxyphenyl)methyl]-1(2*H*)-phthalazinone (56c).** A solution of **56b** diformate (100 mg, 0.13 mmol) in DCM (10 mL) was cooled in an ice-bath under nitrogen and then treated with boron tribromide solution in hexanes (1M, 0.3 mL), followed by another portion (0.3 mL) after 2 h. The mixture stood at room temperature for a total of 2 days and 4 h, and then the solvents were removed under reduced pressure. The residue was dissolved in MeOH−DMSO (1:1, 2 mL) and purified by MDAP to give 18 mg, which was repurified by MDAP to give **56c** (13 mg, 14%) LCMS RT = 2.37 min, 92%, ES+ve $m/z$ 623 $(M + H)^+$, 312 $(M/2 + H)^+$. $^1$H NMR $\delta$ ($CD_3OD$) 8.42 (2H, br s), 8.40−8.37 (1H, m), 8.00 (1H, m), 7.90−7.81 (2H, m), 7.12 (2H, d, $J$ = 8 Hz), 7.07 (2H, d, $J$ = 9 Hz), 6.82 (2H, d, $J$ = 9 Hz), 6.70 (2H, d, $J$ = 8 Hz), 4.60 (2H, m), 4.24 (2H, s), 4.02 (2H, t, $J$ = 6 Hz), 3.45−3.30 (5H, m), 3.20−3.00 (2H, m), 3.11−2.95 (2H, m), 2.54 (2H, t, $J$ = 7 Hz), 2.33−2.16 (4H, m), 2.13−1.88 (8H, m), 1.78−1.58 (8H, m).

**4-[(4-Chlorophenyl)methyl]-2-({(2*R*)-1-[5-(4-{[3-(hexahydro-1*H*-azepin-1-yl)propyl]oxy}phenyl)pentyl]-2-pyrrolidinyl}methyl)-1(2*H*)-phthalazinone (57).** 5-(4-{[3-(Hexahydro-1*H*-azepin-1-yl)propyl]oxy}phenyl)pentyl methanesulfonate (**44**) (142 mg, 0.36 mmol) was stirred with **14** (126 mg, 0.36 mmol) in MeCN (10 mL) at 80 °C under nitrogen containing sodium bicarbonate (60 mg, 0.72 mmol) for six days when reaction appeared almost complete. The mixture was evaporated to dryness, and the residue in DCM was loaded onto a 20 g silica cartridge which had been preconditioned with DCM. The cartridge was eluted with DCM−EtOH−0.88 aq ammonia solution (200:8:1) and then (100:8:1) to give impure product in three fractions (52, 74, and 25 mg). The 74 and 25 mg portions were combined and loaded onto two 20 cm × 20 cm silica preparative plates (1 mm thick layer), which were developed twice in DCM−EtOH−0.88 aq ammonia solution (100:8:1). The main band was taken off and eluted to give **57** (50 mg, 21%). LCMS RT = 2.58 min, 100%, ES+ve $m/z$ 655 $[M + H]^+$, ES+ve $m/z$ 329 $[1/2M + H]^+$. $^1$H NMR ($CDCl_3$) 8.48−8.43 (1H, m), 7.72−7.62 (3H, m), 7.26 (2H, d, $J$ = 8 Hz), 7.20 (2H, d, $J$ = 8 Hz), 7.07 (2H, d, $J$ = 8 Hz), 6.81 (2H, d, $J$ = 8 Hz), 4.43 (1H, dd, $J$ = 4, 13 Hz), 4.25 (2H, s), 4.07 (1H, dd, $J$ = 9, 13 Hz), 4.00 (2H, t, $J$ = 6 Hz), 3.22−3.16 (3H, m), 3.02−2.93 (2H, m), 2.93−2.73 (4H, m), 2.52 (2H, t, $J$ = 7.5 Hz), 2.40−2.29 (1H, m), 2.27−2.18 (1H, m), 2.09−1.98 (2H, m), 1.90−1.68 (8H, m), 1.67−1.53(8H, m), 1.42−1.25 (2H, m). HRMS ES+ve $m/z$: calcd for $C_{40}H_{52}ClN_4O_2$, 655.3779; found, 655.3792.

**4-[(4-Chlorophenyl)methyl]-2-({(2R)-1-[4-(4-{[3-(hexahydro-1*H*-azepin-1-yl)propyl]oxy}phenyl)butyl]-2-pyrrolidinyl}methyl)-1(2*H*)-phthalazinone (56a) from 63.** (Scheme 12) To a solution of 4-[(4-chlorophenyl)methyl]-2-{[(2*R*)-1-(4-{4-[(3-chloropropyl)oxy]phenyl}butyl)-2-pyrrolidinyl]methyl}-1(2*H*)-phthalazinone (**63**) (20 g, 34.6 mmol) in 2-butanone (200 mL) under nitrogen was added potassium iodide (11.5 g, 69.2 mmol), potassium carbonate (9.6 g, 69.2 mmol), and hexamethylene imine (7.8 mL, 69.2 mmol). The reaction mixture was heated at reflux for 41 h. The solid was removed by filtration and washed with 2-butanone (2 × 100 mL). The combined filtrate and washings were evaporated in vacuo, and the residue was dissolved in MeOH−DMSO (1:1; 30 mL). The solution was applied to two C18 reverse phase cartridges (330 g) and eluted using a gradient of 0−50% (MeCN containing 0.05% TFA)−(water containing 0.05% TFA) over 12 CV. The required fractions were evaporated in vacuo, and the residue was dissolved in MeOH. The solution was applied to four amino propyl cartridges (70 g) and eluted with MeOH. The required fractions were evaporated in vacuo to afford **56a** (10.74 g, 48%): LCMS RT = 2.67 min, ES+ve $m/z$ 641/643 $[M + H]^+$. Anal. Chiral HPLC RT = 7.9 min, 100%.

**4-[(4-Chlorophenyl)methyl]-2-({(2*S*)-1-[4-(4-{[3-(hexahydro-1*H*-azepin-1-yl)propyl]oxy}phenyl)butyl]-2-pyrrolidinyl}methyl)-1(2*H*)-phthalazinone (58).** Compound **58** Was prepared from 4-[(4-chlorophenyl)methyl]-2-{[(2*S*)-1-(4-{4-[(3-chloropropyl)oxy]phenyl}butyl)-2-pyrrolidinyl]methyl}-1(2*H*)-phthalazinone (*S*-enantiomer of **63**) by the procedure described above for **56a**, yield (92 mg, 55%). LCMS and $^1$H NMR same as for **51a**. Anal. Chiral HPLC RT = 7.9 min, 2.1% (*R*-isomer) and 10.38 min, 97.9% (*S*-isomer)

## ■ ASSOCIATED CONTENT

**Ⓢ Supporting Information.** Preparative details and spectroscopic data for compounds **3−5**, **8**, **9**, **6**, **14**, **10a**, **11a**, **16**, **18**, **22−27**, **20**, **30−33**, **10b−10d**, **35−37**, **10e−r**, **38−41**, **52**, **53**, **44**, **46**, **47**, **48**, **49**, **43**, **54**, **60−63**, (*S*)-enantiomers of **61−63**, biological screens, table of LCMS purity and retention times, and microanalytical data on **56a**-1,5-naphthalenedisulfonate salt, molecular modeling. This material is available free of charge via the Internet at http://pubs.acs.org.

## ■ AUTHOR INFORMATION

**Corresponding Author**

*Phone: (+44)1438 762883. Fax: (+44)1438 768302. E-mail: pan.a.procopiou@gsk.com.

## ■ ABBREVIATIONS USED

Fluo-4AM, 4-(6-acetoxymethoxy-2,7-difluoro-3-oxo-9-xanthenyl)-4′-methyl-2,2′-(ethylenedioxy)dianiline-*N,N,N′,N′*-tetraacetic acid tetrakis(acetoxymethyl) ester; GTP-$\gamma$-S, guanosine-5′-[$\gamma$-thio]-triphosphate; TBTU, (*O*-benzotriazol-1-yl)-*N,N,N′,N′*-tetramethyluronium tetrafluoroborate

## ■ REFERENCES

(1) Bousquet, J.; Van Cauwnberge, P.; Khaltaev, N. ARIA Workshop Group, World Health Organization. Allergic rhinitis and impact on asthma. *J. Allergy Clin. Immunol.* **2001**, *108*(Suppl 5) S147−S336.

(2) Berger, W. E. Overview of allergic rhinitis. *Ann. Allergy Asthma Immunol.* **2003**, *90*, 7–12.

(3) Leynaert, B.; Neukirch, C.; Liard, R.; Bousquet, J.; Neukirch, F. Quality of life in allergic rhinitis and asthma. A population-based study of young adults. *Am. J. Respir. Crit. Care Med.* **2000**, *162*, 1391–1396.

(4) Bäumer, W.; Rossbach, K. Histamine as an immunomodulator. *JDDG, J. Germ. Soc. Derm.* **2010**, *8*, 495–504.

(5) Simons, F. E. R. $H_1$-antihistamines: more relevant than ever in the treatment of allergic disorders. *J. Allergy Clin. Immunol.* **2003**, *112* (Suppl 4), S42–S52.

(6) Gushchin, I. S. Inverse agonists of $H_1$ receptors as promising antiallergy agents. *Pharm. Chem. J.* **2010**, *44*, 1–6.

(7) Ganellin, C. R. In *Pharmacology of Histamine Receptors*; Ganellin, C. R., Parsons, M. E., Eds.; Wright: Bristol, UK, 1982, pp 11−102.

(8) Sander, K.; Kottke, T.; Stark, H. Histamine $H_3$ receptor antagonists go to clinics. *Biol. Pharm. Bull.* **2008**, *31*, 2163–2181.

(9) Leurs, R.; Blandina, P.; Tedford, C.; Timmerman, H. In *The Histamine H3 Receptor; A Target for New Drugs*, 1st ed.; Leurs, R., Timmerman, H., Eds.; Elsevier: Amsterdam, 1998.

(10) Leurs, R.; Blandina, P.; Tedford, C.; Timmerman, H. Therapeutic potential of histamine $H_3$ receptor agonists and antagonists. *Trends Pharmacol. Sci.* **1998**, *19*, 177–183.

(11) Łażewska, D.; Kieć-Kononowicz, K. Recent advances in histamine $H_3$ receptor antagonists/inverse agonists. *Expert Opin. Ther. Pat.* **2010**, *20*, 1147–1169.

(12) Bhatt, H. G.; Agrawal, Y. K.; Raval, H. G.; Manna, K.; Desai, P. R. Histamine $H_4$ receptor: a novel therapeutic target for immune and allergic responses. *Mini-Rev. Med. Chem.* **2010**, *10*, 1293–1308.

(13) Lehman, J. M.; Blaiss, M. S. Selecting the optimal oral antihistamine for patients with allergic rhinitis. *Drugs* **2006**, *66*, 2309–2319.

(14) Lee, C.; Corren, J. Review of azelastine nasal spray in the treatment of allergic and non-allergic rhinitis. *Expert Opin. Pharmacother.* **2007**, *8*, 701–709.

(15) Bernstein, J. A. Azelastine hydrochloride: a review of pharmacology, pharmacokinetics, clinical efficacy and tolerability. *Curr. Med. Res. Opin.* **2007**, *23*, 2441–2452.
(16) Ishikawa, S.; Sperelakis, N. Histamine $H_3$ receptor-mediated inhibition of noradrenaline release in pig retina discs. *Arch. Pharmacol.* **1987**, *324*, 497–501.
(17) Malinowska, B.; Schlicker, E. $H_3$ receptor-mediated inhibition of neurogenic vasopressor responses in the pithed rats. *Eur. J. Pharmacol.* **1991**, *205*, 307–310.
(18) Hey, J. A.; Del Prado, M.; Egan, R. W.; Kreuter, W.; Chapman, R. W. Inhibition of sympathetic hypertensive responses in the guinea pig by prejunctional $H_3$-receptors. *Br. J. Pharmacol.* **1992**, *107*, 347–350.
(19) Hey, J. A.; Aslanian, R.; Bolser, D. C.; Chapman, R. W.; Egan, R. W.; Rizzo, C. A.; Shih, N.-Y.; Fernandez, X.; McLeod, R. L.; West, R.; Kreutner, W. Studies on the pharmacology of the novel histamine $H_3$ receptor agonist Sch 50971. *Arzneim. Forsch. Drug Res.* **1998**, *48*, 881–888.
(20) Molderings, G. J.; Weissenborn, G.; Schlicker, E.; Likungu, J.; Göthert, M. Inhibition of noradrenaline release from the sympathetic nerves of the human saphenous vein by presynaptic histamine $H_3$ receptors. *Naunyn-Schmiedeberg's Arch. Pharmacol.* **1992**, *346*, 46–50.
(21) Valentine, A. F.; Rizzo, C. A.; Rivelli, M. A.; Hey, J. A. Pharmacological characterization of histamine $H_3$ receptors in human saphenous vein and guinea pig ileum. *Eur. J. Pharmacol.* **1999**, *366*, 73–78.
(22) Varty, L. M.; Hey, J. A. Histamine $H_3$ receptor activation inhibits neurogenic sympathetic vasoconstriction in porcine nasal mucosa. *Eur. J. Pharmacol.* **2002**, *452*, 339–345.
(23) Varty, L. M.; Gustafson, E.; Laverty, M.; Hey, J. A. Activation of Histamine $H_3$ receptors in human nasal mucosa inhibits sympathetic vasoconstriction. *Eur. J. Pharmacol.* **2004**, *484*, 83–89.
(24) McLeod, R. L.; Mingo, G. G.; Herczku, C.; DeGennaro-Culver, F.; Kreutner, W.; Egan, R. W.; Hey, J. A. Combined histamine $H_1$ and $H_3$ receptor blockade produces nasal decongestion in an experimental model of nasal congestion. *Am. J. Rhinol.* **1999**, *13*, 391–399.
(25) McLeod, R. L.; Rizzo, C. A.; West, R. E., Jr.; Aslanian, R.; McCormick, K.; Bryant, M.; Hsieh, Y.; Korfmacher, W.; Mingo, G. G.; Varty, L.; Williams, S. M.; Shih, N.-Y.; Egan, R. W.; Hey, J. A. Pharmacological characterization of the novel histamine $H_3$-receptor antagonist *N*-(3,5-dichlorophenyl)-*N*′-[[4-(1*H*-imidazol-4-ylmethyl)phenyl]-methyl]-urea (Sch 79687). *J. Pharmacol. Exp. Ther.* **2003**, *305*, 1037–1044.
(26) Beaton, G.; Moree, W. J. The expanding role of $H_1$ antihistamines: a patent survey of selective and dual activity compounds 2005–2010. *Expert Opin. Ther. Pat.* **2010**, *20*, 1197–1218.
(27) Taylor-Clark, T.; Sodha, R.; Warner, B.; Foreman, J. Histamine receptors that influence blockage of the normal human nasal airway. *Br. J. Pharmacol.* **2005**, *144*, 867–874.
(28) Aslanian, R.; wa Mutahi, M.; Shih, N.-Y.; Piwinski, J. J.; West, R.; Williams, S. M.; She, S.; Wu, R.-L; Hey, J. A. Identification of a dual histamine $H_1/H_3$ receptor ligand based on the $H_1$ antagonist chlorpheniramine. *Bioorg. Med. Chem. Lett.* **2003**, *13*, 1959–1961.
(29) Procopiou, P. A.; Ancliff, R. A.; Bamford, M. J.; Browning, C.; Connor, H.; Davies, S.; Fogden, Y. C.; Hodgson, S. T.; Holmes, D. S.; Looker, B. E.; Morriss, K. M. L.; Parr, C. A.; Pickup, E. A.; Sehmi, S. S.; White, G. V.; Watts, C. J.; Wilson, D. M.; Woodrow, M. D. 4-Acyl-1-(4-aminoalkoxyphenyl)-2-ketopiperazines as a novel class of non-brain-penetrant histamine $H_3$ receptor antagonists. *J. Med. Chem.* **2007**, *50*, 6706–6717.
(30) Hodgson, S. T.; unpublished results.
(31) Casale, T. B. The interaction of azelastine with human lung histamine $H_1$, $\beta$, and muscarinic receptor-binding sites. *J. Allergy Clin. Immunol.* **1989**, *83*, 771–776.
(32) Fleischhauer, I.; Kutscher, B.; Engel, J.; Achterrath-Tuckermann, U.; Borbe, H. O.; Schmidt, J.; Szelenyi, I.; Camuglia, G. Chirality of azelastin and flezelastine: investigation of their enantiomers. *Chirality* **1993**, *5*, 366–369.
(33) Vogelsang, D.; Scheffler, G.; Brock, N.; Lenke, D.; Vogelsang Schafer, U. Basically substituted benzyl phthalazone derivatives, acid salts thereof and process for the production thereof. U.S. Patent US3813384, 1974.
(34) Scheffler, G.; Engel, J.; Kutscher, B.; Sheldrick, W. S.; Bell, P. Synthesis and X-ray structure analysis of azelastine. *Arch. Pharm.* **1988**, *321*, 205–208.
(35) Engelbrecht, H. J.; Lenke, D.; Muller, H. Aminocarboxylic acid derivatives having antiallergic/antiasthmatic effect and a process for their preparation. German Patent DE1046625, 1958.
(36) Knaak, M.; Fleischhauer, I.; Charpentier, P.; Emig, P.; Kutscher, B.; Müller, A. Ring-rearrangement during the Mitsunobu alkylation of phthalazinones and indazolols. *Liebigs Ann.* **1996**, 1477–1482.
(37) De Camp Schuda, A.; Mazzocchi, P. H.; Fritz, G.; Morgan, T. A Short and Efficient Synthesis of 4,5-Disubstituted-1-pentenes. *Synthesis* **1986**, 309–312.
(38) Sullivan, E.; Tucker, E. M.; Dale, I. L. Measurement of [$Ca^{2+}$] using the Fluorometric Imaging Plate Reader (FLIPR). *Methods Mol. Biol.* **1999**, *114*, 125–133.
(39) Shi, L.; Javitch, J. A. The binding site of aminergic G protein-coupled receptors: the transmembrane segments and second extracellular loop. *Annu. Rev. Pharmacol. Toxicol.* **2002**, *42*, 437–467.
(40) Lin, S. W.; Sakmar, T. P. Specific tryptophan UV-absorbance changes are probes of the transition of rhodopsin to its active state. *Biochemistry* **1996**, *35*, 11149–11159.
(41) Gore, P. M.; Hancock, A. P.; Hodgson, S. T.; Kindon, L. J.; Procopiou, P. A. 2-Substituted 4-benzylphthalazinone derivatives as histamine H1 and H3 antagonists. Patent WO 2007122156 A1 1 Nov 2007.
(42) Yi, C.-S.; Martinelli, L. C.; Blanton, C.; DeWitt, Jr. Synthesis of *N*-methyl-1-oxa-5-aza[10]paracyclophane: a conformationally restricted analog of phenoxypropylamines. *J. Org. Chem.* **1978**, *43*, 405–409.
(43) Strogryn, E. L. New synthesis of antimalarials related to 2-bromo-4,5-dimethoxy-*N*,*N*-bis(diethylaminoethyl)aniline. Terminal nitrogen modifications. *J. Med. Chem.* **1970**, *13*, 864–866.
(44) Slack, R. J.; Russell, L. J.; Hall, D. A.; Luttmann, M. A.; Ford, A. J.; Saunders, K. A.; Hodgson, S. T.; Connor, H. E.; Browning C.; Clark, K. L. Pharmacological characterisation of GSK1004723, a novel, long acting antagonist at histamine $H_1$ and $H_3$ receptors. *Br. J. Pharmacol.*, in press.